Optical Engineering

OpticalEngineering.SPIEDigitalLibrary.org

Temperature analysis of Cassegrain optical antenna for space laser communication

Yiyi Zhao
Xiaolong Ma
Bin Xue
Fu Li
Yinghong He
Juan Lv
Xingtao Yan
Jirui Yu
Meng Xiang

SPIE.

Yiyi Zhao, Xiaolong Ma, Bin Xue, Fu Li, Yinghong He, Juan Lv, Xingtao Yan, Jirui Yu, Meng Xiang, "Temperature analysis of Cassegrain optical antenna for space laser communication," *Opt. Eng.* **57**(7), 076103 (2018), doi: 10.1117/1.OE.57.7.076103.

Temperature analysis of Cassegrain optical antenna for space laser communication

Yiyi Zhao, Xiaolong Ma, Bin Xue, Fu Li, Yinghong He, Juan Lv, Xingtao Yan, Jirui Yu, and Meng Xiang*
Chinese Academy of Sciences, Xi'an Institute of Optics and Precision Mechanics, Xi'an, China

Abstract. The thermal stability of optical antennas is a key parameter determining the performance of satellite optical communication links. The effects of uniform temperature changes on the performance of a Cassegrain optical antenna are discussed. In addition, a simple theoretical model is proposed to describe the defocusing distance and wavefront aberration (power) as a function of temperature. Through the theoretical model, the thermal stability can be quickly assessed in the optical design stage. The alignment data and thermal experimental results are consistent with the theoretical model. [DOI: 10.1117/1.OE.57.7.076103]

Keywords: thermal effects; telescopes; optical communications; optical antenna.

Paper 180385 received Mar. 25, 2018; accepted for publication Jun. 28, 2018; published online Jul. 23, 2018.

1 Introduction

Satellite laser communication links have several advantages over traditional radio frequency systems, such as extremely high-data rates, small size and mass, low-power consumption, and strong security.[1] At present, laser communication has developed into a promising alternative for space-borne high-speed communication links, and its study has led to an explosive trend in the ongoing and planning projects of many countries.[2–4]

The optical antenna is a key component of the laser communication system. It is an afocal telescope with both receiving and transmitting functions. In the on-orbit state, the space environment directly affects the optical antenna, causing changes in the optical antenna operating temperature and resulting in optical system deformation, which significantly affects the communication quality.[5,6] For the transmitting function, temperature variations can cause changes in the divergence angle of the transmitted laser beam and affect the transmitter gain. For the receiving function, temperature variations can cause a defocus of the signal and beacon beam. The optical intensity distributions focused on the acquisition and tracking sensors degrade because of the defocus caused by temperature variations. Some optical antennas in satellites have stringent thermal control requirements. For example, the SOUT laser communication terminal developed by ESA requires a thermal control accuracy of ±2.5°C at all times and a short temperature change of less than 0.5°C.[7] The Cassegrain optical antenna of the lunar laser communication demonstration developed by NASA requires a thermal control accuracy of ±1°C.[8] However, these control strategies will result in an increase in power consumption and volume.

Spacecraft telescopes typically require several iterative calculations of the optomechanical simulation and finite-element analysis to determine the temperature range. In this study, a theoretical model that can quickly assess the thermal stability of the optical antenna in the optical design stage is developed, the corresponding simulation is carried out, and the experimental results are found to agree with the theoretical simulation results.

*Address all correspondence to: Meng Xiang, E-mail: ningzi0210@126.com

2 Theoretical Analysis

We have developed a 150-mm aperture diameter Cassegrain-type afocal telescope as a spacecraft optical antenna. The antenna consists of an object lens and eye lens, and the object lens consists of a primary mirror and secondary mirror, as shown in Fig. 1.

Many studies have shown that the temperature variation of the Cassegrain object lens produces a purely focal shift with little additional aberration.[9–11] Therefore, we concentrate on the defocus, which makes as the main research direction. In the Cassegrain optical antenna, the focal point of the objective lens and eye lens coincides with each other, and the outgoing light and incident light are parallel beams. However, when the temperature changes, the focus of the objective lens and eye lens no longer coincides, or the eyepiece is out-of-focus, which will cause the transmitting beam and receiving beam to no longer be parallel. The afocal-type design will lead to a higher temperature sensitivity.

2.1 *Factors of Temperature Variation*

Temperature variations can significantly influence the properties of the optical elements and cause (1) variations in the curvature of the primary mirror ΔR_P, (2) variations in the thickness between the primary and secondary mirrors δL, (3) variations in the conjugate distance of the secondary mirror Δ_S, and (4) variations in the back focal length (BFL) of the eye lens Δ_E. These are the main factors that affect the optical performance by temperature change. The first three factors lead to a change in the BFL of the object lens. Thus, the defocusing distance of the antenna Δ can be given by

$$\Delta = \Delta_O + \Delta_E = \Delta_P + \Delta_L + \Delta_S + \Delta_E, \quad (1)$$

where Δ_O is the object lens focal shift, Δ_P is that caused by the primary mirror, and Δ_L is that caused by the thickness between the primary and secondary mirrors.

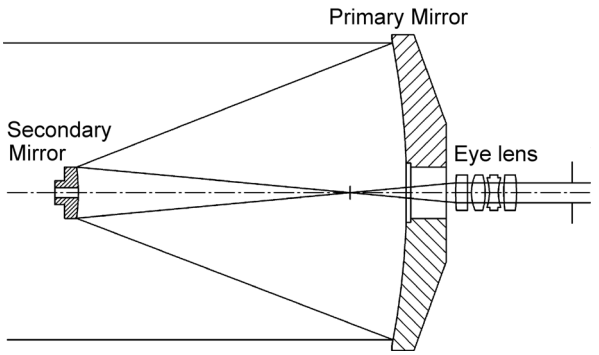

Fig. 1 Optical design of the 150-mm optical antenna.

For ΔR_P, Applewhite determined by finite-element analysis that the radius of the primary mirror changes in a near-linear fashion with the variation in temperature.[9] Baeva et al.[10] provided an experience formula to estimate the variation in the radius of the primary mirror with backside support:

$$\Delta R_P \approx \alpha_P \frac{R_P}{2}\left(1+\frac{R_P}{b}\right)\delta t, \tag{2}$$

where α_P is the linear expansion coefficient of the primary mirror, R_P is the radius of the primary mirror, b is the thickness of the primary mirror, and δt is the variation in temperature.

This factor will be magnified by the secondary mirror, so Δ_P can be expressed as follows:

$$\Delta_P = \beta^2 \Delta R_P = \beta^2 \alpha_P \frac{R_P}{2}\left(1+\frac{R_P}{b}\right)\delta t, \tag{3}$$

$$\beta = \frac{1+e}{1-e}, \tag{4}$$

where β and e are the lateral magnification and eccentricity of the secondary mirror, respectively.

For δL, the variation in thickness between the primary and secondary mirrors can be expressed as follows:

$$\delta L = \alpha_L L \delta t, \tag{5}$$

where α_L is the linear expansion coefficient of the housing between the primary mirror and second mirror.

This factor will also be magnified by the secondary mirror:

$$\Delta_L = \beta^2 \delta L = \beta^2 \alpha_L L \delta t. \tag{6}$$

For Δ_S, the variation in the conjugate distance of the secondary mirror can be calculated from[12]

$$\Delta_S = 2\alpha_S a \beta \delta t, \tag{7}$$

where α_S and a are the linear expansion coefficient and semi-major axis of the secondary mirror, respectively. The smaller the size of the mirror, the weaker the thermal influence.[3] The thermal deformation of the secondary mirror is very small for its small size; so, factor [Eq. (3)] has little effect on the system.

For Δ_E, the focal shift of the refraction system caused by the temperature is linear in a certain temperature range and will be very small or even zero by the appropriate use of material and allocation of focal power; thus, Δ_E can be expressed as follows:

$$\Delta_E = \alpha_E \delta t, \tag{8}$$

where α_E is the linear coefficient of the eye lens and depends on the material used and allocated focal power.

Substituting Eqs. (3), (6)–(8) into Eq. (1), the defocusing distance of the antenna Δ can be given by

$$\Delta = \left[\beta^2 \alpha_P \frac{R_P}{2}\left(1+\frac{R_P}{b}\right) + \beta^2 \alpha_L L + 2\alpha_S a\beta + \alpha_E\right]\delta t. \tag{9}$$

2.2 *Power and Defocusing Distance*

Wavefront aberration is an effective way to assess the defocus effect, which can be measured by a laser interferometer. The wavefront aberration consists of several terms, one of which represents the defocus aberration, which is referred to as "power" in the Seidel polynomials. The power result is derived from a best-fit spherical surface of the wavefront and is equal to the peak-to-valley (PV) value of the defocus wavefront aberration, as shown in Fig. 2. The power is positive for a concave surface and negative for a convex surface. In the Zernike polynomials, the fourth term Z_3 represents the defocus aberration, which is equal to half the power. Simultaneously, the ratio of the RMS to PV defocus wavefront aberration (power) is ~0.286.[13] Therefore, the variation in the RMS wavefront error can be calculated by the variation in power.

Figure 3 illustrates the geometrical relationships of f, D, the defocusing distance, and power, where f is the focal length of the eye lens, l is the distance from the principal plane of the eye lens to the focal point of the objective lens, Δ is the defocusing distance of the eye lens, l' is the BFL after the eye lens is defocused, and W is the power of the wavefront aberration.

From Fig. 3, the following relationship can be obtained:

$$l = f + \Delta, \tag{10}$$

$$\frac{1}{l'} + \frac{1}{l} = \frac{1}{f}, \tag{11}$$

$$W = -\left[l' - \sqrt{l'^2 - (D/2)^2}\right]. \tag{12}$$

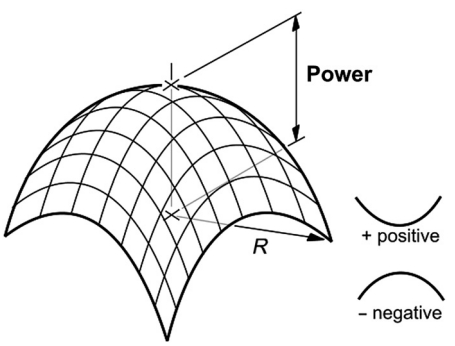

Fig. 2 Power of the wavefront.

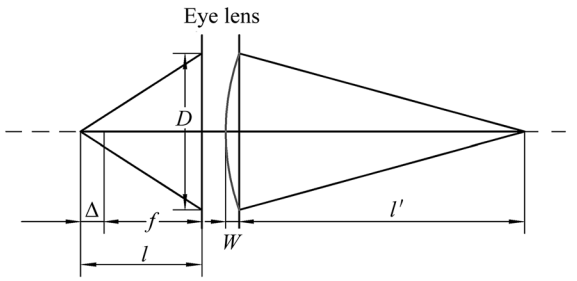

Fig. 3 Relationship between defocusing distance and power.

According to the above equations, we can obtain as follows:

$$W = \sqrt{\left[\frac{f(f+\Delta)}{\Delta}\right]^2 - \left(\frac{D}{2}\right)^2} - \frac{f(f+\Delta)}{\Delta}. \tag{13}$$

As Δ is much smaller than f, the power can be approximately expressed as a linear function of Δ:

$$W = \frac{-(D/2)^2\Delta}{\sqrt{[f(f+\Delta)]^2 - (D/2)^2\Delta} + f(f+\Delta)} \approx -\frac{D^2}{8f^2}\Delta. \tag{14}$$

This relationship is also applicable to the object lens. The linear coefficient of this solution is only relevant to the relative aperture D/f, and the power value measured at the eye lens side and object lens side must be identical.

The relation between the defocusing distance and temperature shift and the approximate linear function relation between the power and defocusing distance can be obtained from Eqs. (9) and (14), respectively. Through these two equations and optical parameters, it is easy to estimate the power of the system with the temperature shift. Simultaneously, the ratio of the RMS defocus wavefront aberration to power is ~0.286, so the effect of temperature on the RMS wavefront error can be further estimated.

3 Theoretical Calculation

For the optical antenna we developed, the material of the primary mirror and secondary mirror is Zerodur, that of the housing between the primary mirror and secondary mirror is invar, and the primary mirror is back-supported. The values of the parameters in Eq. (9) are $R_P = 400$ mm, $\alpha_P = \alpha_S = 0.05 \times 10^{-6}$, $b = 20$ mm, $e = 1.658$, $\alpha_L = 0.7 \times 10^{-6}$, $L = 166$ mm, $a = 51.738$ mm, and $\beta = -4.04$. The eye lens is athermally designed, so Δ_E is very small and approximately zero. We can then obtain as follows:

$$\Delta = 5.30 \times 10^{-3}\delta t. \tag{15}$$

For the developed optical antenna, the values of the parameters in Eq. (14) are $D = 10$ mm and $f = 54$ mm, and we can obtain as follows:

$$W \approx -6.77\Delta\lambda. \tag{16}$$

According to Eqs. (15) and (16), we can obtain the power of the system with the temperature shift:

$$W \approx -0.036\lambda\delta t. \tag{17}$$

4 Alignment and Experiment

4.1 *Alignment*

The axial distance of the object lens and eye lens has an important influence on the emitting and receiving performance of the system. The laser interferometer is an effective instrument to measure and adjust the axial distance and commonly functions at 632.8 nm. However, when the working wavelength of the interferometer and optical antenna is different, the operation of the interferometer becomes difficult. Equation (14) describes the relationship between the power and defocusing distance, which is a key to address this problem.

In our system, the optical antenna is set to 830 nm for tracking and 1550 nm for communication, and the chromatic aberration is corrected for these two wavelengths. The eye lens is also optimized at 632.8 nm, which is used for alignment and testing by the laser interferometer. At the same time, the axial color of the eyepieces at 632.8 nm is not corrected; therefore, the eye lens has a 0.66-mm focal shift at 632.8-nm relative to 1550 and 830 nm. Further, this focal shift corresponds to a -4.5λ ($\lambda = 632.8$ nm) power, calculated by Eq. (16). This implies that if the optical antenna is not defocused at 830 and 1550 nm, the antenna will have a power of -4.5λ at 632.8 nm. This forms the basis for alignment: the power value of the antenna at 632.8 nm should be adjusted to -4.5λ by changing the thickness of the eye lens spacer ring (which determines the axial distance of the object lens and eye lens) to prevent any out-of-focus regions at 830 and 1550 nm using the laser interferometer.

Three eye lens spacers with different thicknesses were tested in the alignment. The system wavefronts under different spacer thicknesses were measured, as shown in Figs. 4 and 5. The variation in spacer thickness is equal to the variation in defocusing distance.

According to the linear fit of the power and spacer thickness, as shown in Fig. 5, the coefficient between the power variation and spacer thickness variation can be obtained: −6.72. This coefficient obtained from the experimental fitting is slightly different from the theoretical value of −6.77 obtained by Eq. (16). This is because: (1) the theoretical value is the approximate value obtained under the condition that the defocusing distance is close to zero and (2) the antenna has an alignment error. Equation (14) and the experiment indicate that the power will change in the negative direction when the spacer thickness increases, and the variation in spacer thickness is −6.72 times the variation in power. According to the above principles, it can be calculated that the power value of the antenna at 632.8 nm will be -4.5λ when the spacer thickness is 2.85 mm. Figure 6 shows the wavefront of the optical antenna when the spacer thickness is 2.85 mm, and it agrees with the theoretical results. The ideal thickness of the spacer can be accurately calculated through only one spacer trial assembly using Eq. (14) to avoid processing several test space rings.

The changes in temperature, defocusing distance, and power can be predicted by Eqs. (9) and (14), and it is possible to guide the assembly to achieve precise alignment of any best operating temperature of the antenna system using the conventional-wavelength (632.8 nm) interferometer at room temperature. This indicates that we can even use the 632.8-nm interferometer at room temperature to align the optical antenna without defocus at any temperature and wavelength.

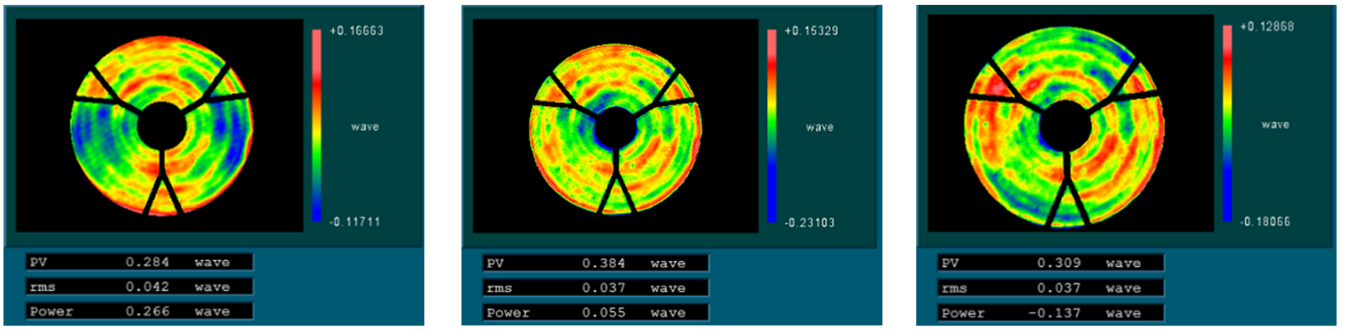

(a) (b) (c)

Fig. 4 Wavefronts under different spacer thicknesses: (a–c) 2.14, 2.17, and 2.20 mm, respectively.

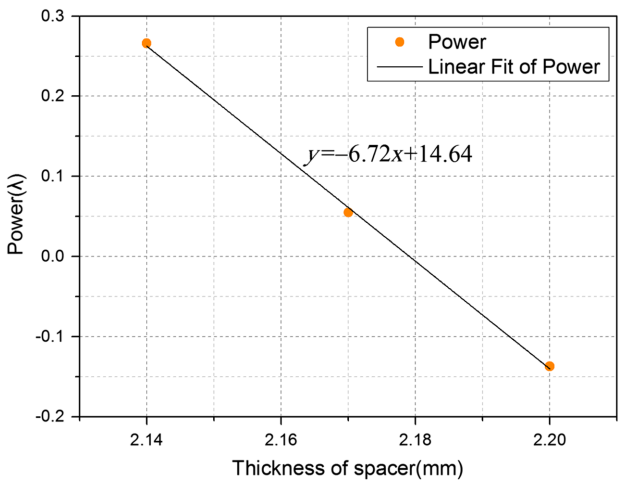

Fig. 5 Linear fit of power and spacer thickness.

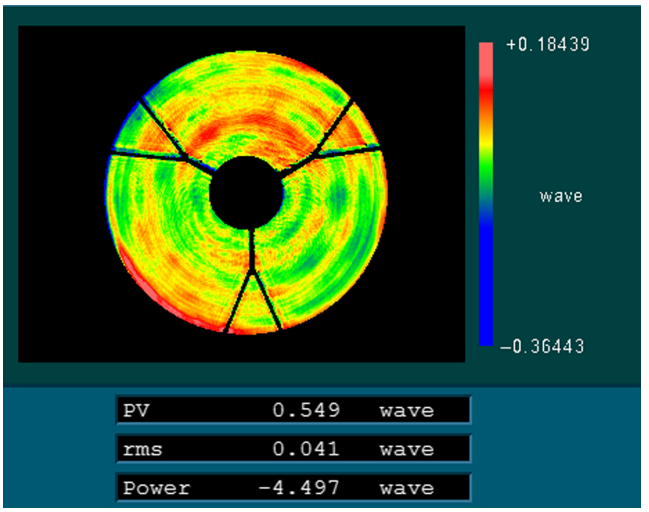

Fig. 6 Wavefront when the spacer thickness is 2.85 mm.

4.2 *Temperature Experiment*

In order to verify the stability of the optical antenna and the above theory, the wavefront aberration of the optical antenna was measured at 15°C to 31°C. The wavefront measurement results at different temperatures are presented in Table 1.

Figure 7 presents the linear fit to the power and temperature. Through the fitting data in Fig. 7, we can conclude that the variation in power is −0.0387 times the variation in temperature, which is very close to the theoretical value of −0.036 obtained by Eq. (16).

The coefficient of power variation with the temperature shift of another optical antenna with the same optical parameter is −0.053. This is because the primary mirror of this optical antenna was not perfectly assembled. The glue dots that used to hold the back of the primary mirror were not uniform, so the temperature variation caused astigmatism and a greater defocus. The coefficient varied to −0.041 after the optical antenna was reassembled. This value is 14% greater than the theoretical value −0.036.

Due to the bonding error, the coefficient of power variation with the temperature has changed by 30% before and after reassemble. The bonding error often causes large astigmatism of the primary mirror, and in some cases, astigmatism even doubles the surface figure error of the primary mirror. Astigmatism indicates that the primary mirror is subjected to inhomogeneous stress. When the temperature changes, the surface figure of the astigmatic primary mirror changes due to the change of stress, resulting in greater fluctuations in the power than the theoretical value. The stress change of the astigmatic primary mirror is almost unpredictable; so, our method does have a large error in the presence of astigmatism. However, the astigmatism of the primary mirror is usually controlled to very small during assembly. After reassembling, there is still a 14% deviation from the theoretical value, which is due to: (a) power is a PV value, and its fluctuation is relatively large; (b) the linear expansion coefficient of the material used for theoretical calculation has a certain error; and (c) the primary mirror still has very small astigmatism.

Table 1 Experimental results of power values at different temperatures (15°C to 31°C).

Temperature (°C)	15	17	19	21	23	25	27	29	31
Power (λ)	−4.892	−4.810	−4.77	−4.638	−4.588	−4.526	−4.413	−4.341	−4.289

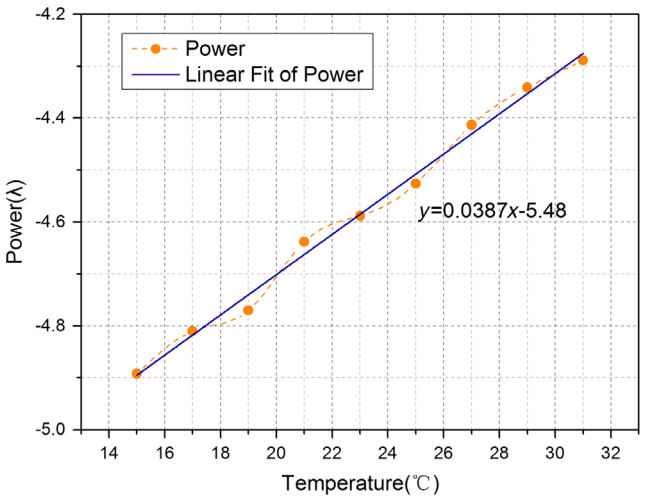

Fig. 7 Linear fit of power and temperature.

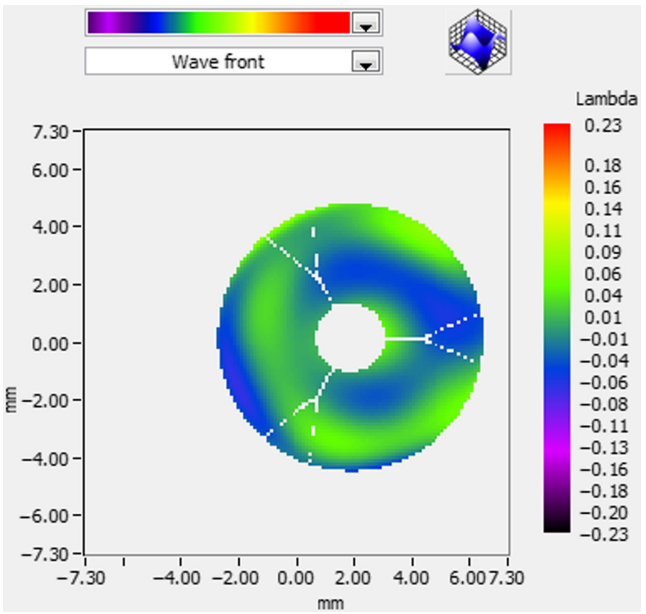

Fig. 8 Wavefronts measured by Shack–Hartmann wavefront sensor.

Although the accuracy of the theoretical analysis results will be affected by the assembled state and may be worse than the finite-element analysis, the thermal stability can be quickly assessed by the above theoretical model in the optical design stage. The calculation error of the theoretical model is primarily due to the assembly condition of the primary mirror. The thermal stability can be accurately calculated if the theoretical analysis combines the finite-element analysis of only the primary mirror instead of the whole system, which will greatly improve the efficiency of the optical antenna design.

Finally, the Shack–Hartmann wavefront sensor was used to measure the wavefront error of the optical antenna at 830 nm. The measurement results at room temperature are presented in Fig. 8; the RMS wavefront error of the optical antenna is 0.029λ and the fourth term of the Zernike polynomials Z_3 is 0.012λ. This indicates that the system exhibits almost no defocus at 830 nm, which verifies the assembly method proposed in Sec. 4.1.

5 Conclusion

In this paper, a theoretical model for evaluating the thermal stability of a Cassegrain optical antenna is proposed. A linear relationship of the defocusing distance and temperature variation of the Cassegrain optical antenna and that of the power and defocusing distance was developed. Using these relationships, the thermal stability can be quickly assessed in the optical design stage without performing several iterative calculations of the optomechanical simulation and finite-element analysis. The predictions of the defocusing distance and power based on this model are also used to precisely connect the object lens and eye lens. The temperature experiment proved that the theoretical model is sufficiently accurate.

Acknowledgments

This work was supported by the West Light Foundation of the Chinese Academy of Sciences (Grant No. XAB2016B27) and the National Natural Science Foundation of China (NSFC) (Grant No. 61505245).

References

1. M. Toyoshima and Y. Takayama, "Space-based laser communication systems and future trends," in *Conf. on Lasers and Electro-Optics, OSA Technical Digest (online)*, Paper JW1C.2, Optical Society of America (2012).
2. A. Carrasco-Casado et al., "LEO-to-ground polarization measurements aiming for space QKD using Small Optical TrAnsponder (SOTA)," *Opt. Express* **24**(11), 12254–12266 (2016).
3. B. Edwards et al., "Overview of the laser communications relay demonstration project," in *SpaceOps 2012 Conf.* (2012).
4. E. Fischer et al., "Advanced optical solutions for inter-satellite communications," *Optik* **112**(9), 442–448 (2001).
5. D. Vukobratovich, "Ultra-lightweight optics for laser communications," *Proc. SPIE* **1218**, 178–192 (1990).
6. L. Tan et al., "Pointing error due to temperature distribution of SiC reflectors in intersatellite laser communications," *Appl. Opt.* **49**(22), 4168–4174 (2010).
7. G. Baister et al., "The SOUT optical intersatellite communication terminal," in *Proc. of IEEE Conf. on Optoelectronics*, pp. 345–355, IEEE (1994).
8. J. W. Burnside et al., "Design of an inertially stabilized telescope for the LLCD," *Proc. SPIE* **7923**, 79230L (2011).
9. R. W. Applewhite, "The effects of thermal gradients on the Mars Observer Camera Primary Mirror," *Proc. SPIE* **1690**, 376–386 (1992).
10. Y. V. Baeva, E. V. Lapovok, and S. I. Khankov, "Longitudinal thermo-optical aberration of the image in reflective telescopes," *J. Opt. Technol.* **80**(1), 148–153 (2013).
11. G. Zheng et al., "Influence of temperature on divergence angle of a focal telescope used in laser optical communication," *Opt. Express* **20**(12), 13208–13214 (2012).
12. K. I. Abdusamatov and S. I. Khankov, "Calculating the thermal aberrations of a space-based solar telescope-limbograph," *J. Opt. Technol.* **73**(1), 24–28 (2013).
13. R. R. Shannon, *The Art and Science of Optical Design*, Chapter 4, Cambridge University, Cambridge, United Kingdom (1997).

Yiyi Zhao is a research associate at Xi'an Institute of Optics and Precision Mechanics of Chinese Academy of Sciences. He received his BS degree from China Jiliang University in 2010 and his PhD in optical engineering from the University of Chinese Academy of Sciences in 2015. His current research interests include optical design and space laser communication.

Xiaolong Ma is an associate professor at Xi'an Institute of Optics and Precision Mechanics of Chinese Academy of Sciences. He received his BS degree from Northwestern University in 1996 and his master's degree in optical engineering from the University of Chinese Academy of Sciences in 2006. His current research interests include optical design and space laser communication.

Bin Xue is a professor at Xi'an Institute of Optics and Precision Mechanics of Chinese Academy of Sciences. He received his BS degree from Xidian University in 2001 and his PhD in optical engineering from the University of Chinese Academy of Sciences in 2006. His current research interests include optical system design and spectral imaging technology.

Fu Li is a professor at Xi'an Institute of Optics and Precision Mechanics of Chinese Academy of Sciences. He received his BS degree from Taiyuan University of Technology in 2001 and his PhD in optical engineering from the University of Chinese Academy of Sciences in 2006. His current research interests include optomechanical system design and space laser communication.

Yinghong He is an associate professor at Xi'an Institute of Optics and Precision Mechanics of Chinese Academy of Sciences. She received her BS degree from Xi'an Technology University in 1998 and her master's degree in optical engineering from the Sichuan University in 2004. Her current research interests include optical design and space laser communication.

Juan Lv is an associate professor at Xi'an Institute of Optics and Precision Mechanics of Chinese Academy of Sciences. She received her BS and master's degree from Xidian University. Her current research interests include optical design and space laser communication.

Xingtao Yan is an associate professor at Xi'an Institute of Optics and Precision Mechanics of Chinese Academy of Sciences. He received his BS and master's degree from Xidian University. His current research interests include optical design and space laser communication.

Jirui Yu is a research associate at Xi'an Institute of Optics and Precision Mechanics of Chinese Academy of Sciences. He received his BS degree from Xi'an Jiaotong University in 2011 and his master's degree from the Zhejiang University in 2015. His current research interests include optomechanical system design and space laser communication.

Meng Xiang is a PhD candidate in Xi'an Institute of Optics and Precision Mechanics. She received her master's degree from Xi'an Institute of Optics and Precision Mechanics of Chinese Academy of Sciences in 2015. Her research direction is optical design.